Appendix D

Magnitude and Area Data for Strike Slip Earthquakes

William L. Ellsworth
U.S. Geological Survey
Menlo Park, CA

This appendix contains a compilation of data sets on the magnitudes and dimensions of large-magnitude strike slip earthquakes. The data sets consists of:

Table D.1. Fifty two earthquakes from Wells and Coppersmith (1994). These events range in **M** from 5.55 to 7.9. They include only those events from Table 1 of Wells and Coppersmith (1994) that those authors considered reliable enough to include in their regression analysis.

Table D.2. Seven California earthquakes for which surface ruptures and/or geodetic models are available in the literature. These events range in **M** from 6.95 to 7.88, and include multiple estimates of **M** and rupture dimensions for 4 of the events.

Table D.3. Eight earthquakes with slip models determined from inversion of seismograms, as interpreted by Sommerville, et al. (1999). In their interpretation of the published slip models, the authors trimmed some area from the slip models. These events range in **M** from 5.66 to 7.22.

Table D.4. Nineteen events compiled from new (and a few unpublished) sources. These events range in **M** from 6.5 to 8.1. The source parameters are determined from available geologic, geodetic and seismological data. Five of the events have more than one estimate of their parameters. Many of the added events are 20th century earthquakes that are listed in Table 1 of Wells and Coppersmith (1994), and that have revised or improved information based on new analyses and data.

The length (L) and width (W) of the ruptures are given in km. Seismic moments are in dyne-cm, with a shear modulus of 3_10^{11} dynes/cm2. All magnitudes are moment magnitudes (**M**). The number of measurements for earthquakes with **M**‡ 7 in the combined data set has increased to 37 from the 11 included in Wells and Coppersmith (1994).

Measurement uncertainty in M and A

Multiple estimates of L, W, A and **M** are available for 16 earthquakes in the combined data set. These redundant measurements can be used to estimate the errors associated with measuring **M** and A. If we consider the difference in magnitude between all possible pairs that measure the same earthquake, an estimated standard deviation (s.d.) of 0.08 magnitude units is obtained for **M**. Similarly, the standard deviation of the ratio of A between pairs of estimates is 1.4 (or 0.15 log-units). Thus, there is significant uncertainty in the data that goes into the correlation analysis.

Regression models of M(A)

Relations between the data in Tables D.1-D.4 are displayed in several different formats in Figures 1-3. These data show a clear dependence of moment magnitude on area (A) (Figure D.1), and of mean slip (U) on **M** (Figure D.2) and on rupture length (Figure D.3). Note in particular that mean slip increases as the fault length grows. This suggests that stress drop should also increase with increasing fault length. Stress drop can be approximately determined from these data using equation 31 of Chinnery (1969). This equation can be used to derive the stress drop at the center of a rectangular dislocation with constant slip that intersects the free surface. These data do indeed show an increase in stress drop with increasing rupture length (Figure D.4).

In principal, the data in Figure D.1 provide all of the information needed to define a **M**(A) relationship. Rather than simply apply the least-squares method, a robust regression method is used that is insensitive to data outliers (Rousseeuw and Leroy, 1987). This is preferable, because we do not have very good control on the errors in the data from the tables. The results of fitting a log-linear regression model to all of the data is

$$\mathbf{M} = 4.17 + 1.015 \log_{10}(A).$$

If we insist on d=1, the best fitting model is

$$\mathbf{M} = 4.16 + \log_{10}(A).$$

If we further restrict the fit to $A>500\ km^2$

$$\mathbf{M} = 4.20 + \log_{10}(A).$$

This fit has an r.m.s. error of 0.19.

Similarly, the best model with d=4/3 for $A>500\ km^2$ is

$$\mathbf{M} = 3.1 + 4/3 \log_{10}(A).$$

This fit has an r.m.s. error of 0.21. The last two equations are essentially identical to equations (2.6b) and (2.8b).

Aleatory variability of M given A

How much variability in **M** occurs when two strike slip faults with identical lengths break, or when the same earthquake happens repeatedly? In other words, how much aleatory variation in **M** is to be expected given that a rupture with area A occurs. This question is difficult to answer from data, as the measurement of both **M** and A are subject to measurement uncertainty.

To approach this question, consider the hypothetical rupture of each of the 38 WG99 rupture sources, producing an earthquake with magnitude given by $\mathbf{M} = 4.2 + \log_{10}(A)$. Further suppose that when we observe each event that our measurements of A and **M** are uncertain by the same s.d. derived from the comparison of multiple estimates of actual earthquakes discussed above. We can then plot the estimated **M** versus A just as was done in Figure D.1. Figure D.5 shows the result. By construction, the true data that underlie the figure fall on the theoretical (solid) line. The scatter in the points is purely due to measurement error.

Figure D.5 also contains two pairs of lines that correspond to the 90% range for Gaussian variability in **M** about the true A for two different s.d.(**M**). The narrower range (dashed lines) corresponds to s.d.(**M**)=0.12, and the wider range (dotted lines) is for s.d.(**M**)=0.25. Suppose that these two ranges correspond to proposed the intrinsic (aleatory) variation in **M** given A. Clearly, the case with s.d.(**M**)=0.25 is inconsistent with the data, while the narrower range would be difficult to reject.

Now compare Figures D.1 and D.5 (they are plotted on the same axes and scale, and can be overlaid). There are two points to be taken from their obvious similarity. First, simple estimates of measurement uncertainty in A and **M** derived from multiple observations of the same earthquakes produce scatter in the otherwise exact data in Figure 4.5 that roughly mimics the behavior of the actual data in Figure D.1. Second, aleatory variability in **M**(A) of s.d.(**M**)=0.12 magnitude units lies comfortably within the scatter of the data. Given the estimated errors in the measured **M** and A, aleatory variability of 0.12 in **M** is consistent with the actual data in Figure D.1. However, a larger value such as s.d.(**M**)=0.25 would be inconsistent with the data, as the 90% range exceeds the range of the observations in Figure D.1.

References

Aky z, H.S., Barka. A., Altunel, E., Hartleb, R., and Sunal, G., 2000, Field observations and slip distribution of the November 12, 1999 Duzce earthquake (M=7.1), Bolu — Turkey: The 1999 Izmit and D zce Earthquakes: preliminary results, Barka, A., Kozaci, , Aky z, and Altunel, E., eds., Instanbul Technical University, p. 63-70.

Arnadottir, T., Segall, P., and Matthews, M., 1992, Resolving the discrepancy between geodetic and seismic fault models for the 1989 Loma Prieta, California, earthquake: Bulletin of the Seismological Society of America, v. 82, p. 2248-2255.

Barka, A.A., 1996, Slip distribution along the North Anatolian Fault associated with the large earthquakes pf the period 1939 to 1967: Bulletin of the Seismological Society of America, v. 86, p. 1238-1254.

Beanland, S., and Clark, M.M., 1994, The Owens Valley Fault Zone, eastern California, and surface faulting associated with the 1872 earthquake: U.S. Geological Survey Bulletin, Report B, 1982.

Chinnery, M.A., 1969, Theoretical fault models: Dominion Observatory Ottawa Publications, v. 37, p. 211-223.

Delouis, B., Lundgren, P., Salichon, J., and Giardini, D., 2000, Joint inversion of InSAR and teleseismic data for the slip history of the 1999 Izmit (Turkey) earthquake: Geophysical Research Letters, v. 27, p. 3389-3392.

Freymuller, J., King, N.E., and Segall, P., 1994, The co-seismic slip distribution of the Landers earthquake: Bulletin of the Seismological Society of America, v. 84, p. 646-659.

Hudnut, K.W., Bock, Y., Cline, M., Fang, P., Feng, Y., Freymuller, J., Ge, X., Gross, W.K., Jackson, D., Kim, M., King, N.E., Langbein, J., Larsen, S.C., Lisowsik, M., Shen, Z.-K., Svarc, J., and Zhang, J., 1994, Co-seismic displacements of the 1992 Landers earthquake sequence: Bulletin of the Seismological Society of America, v. 84, p. 625-645.

Ji, C., Wald, D.J., and Helmberger, D.V., in press, Source description of the 1999 Hector Mine, California, earthquake: Part II: complexity of the slip history: Bulletin of the Seismological Society of America.

King, N.E., and Thatcher, W., 1998, The coseismic slip distribution of the 1940 and 1979 Imperial Valley, California, earthquakes and their implications: Journal of Geophysical Research, v. 103, p. 18,069-18,086.

Lisowski, M., Prescott, W.H, Savage, J.C., and Johnston, M.J.S., 1990, Geodetic estimate of the coseismic slip during the 1989 Loma Prieta, California, earthquake: Geophysical Research Letters, v. 17, p. 1437-1440.

Molnar. P., and Chen, W.P., 1977, Seismic moments of major earthquakes and the average rate of slip in Central Asia: Journal of Geophysical Research, v. 82, p. 2945-2969.

Peltzer, G., Crampe, F., and King, G.,1999, Evidence of nonlinear elasticity of the crust from the M_W 7.6 Manyi (Tibet) earthquake: Science, v. 286, p. 272-276.

Rousseeuw, P.J., and Leroy, A.M., 1987, Robust Regression and Outlier Detection: John Wiley and Sons, New York.

Sieh, K., 1978, Slip along the San Andreas Fault associated with the great 1857 earthquake: Bulletin of the Seismological Society of America, v. 68, p. 1421-1448.

Sommerville, P., Irikura, K., Graves, R., Sawasa, S., Wald, D., Abrahamson, N., Iwasaki, Y., Kagawa, T., Smith, N., and Kowada, A., 1999, Characterizing crustal earthquake slip models for prediction of strong ground motion: Seismological Research Letters, v. 70, p. 59-80.

Stein, R.S., Barka, A.A., and Dieterich, J.H., 1997, Progressive failure on the North Anatolian fault since 1939 by earthquake stress triggering: Geophysical Journal International, v. 128, p. 594-604.

Stein, R.S., and Hanks, T.C., 1998, M ‡ 6 earthquakes in southern California during the twentieth century: no evidence for a seismicity or moment deficit: Bulletin of the Seismological Society of America, v. 88, p. 635-652.

Thatcher, W., Marshall, G., and Lisowsik, M,1997, Resolution of fault slip along the 7\470-km-long rupture of the great 1906 earthquake and its implications: Journal of Geophysical Research, v. 102, p. 5353-5367.

Wells, D.L., and Coppersmith, K.J., 1994, New empirical relationships among magnitude, rupture length, rupture width, rupture area, and surface displacement: Bulletin of the Seismological Society of America, v. 84, p. 974-1002.

Wright, T., Parsons, B., and Fielding, E., 2001, Triggered slip, observations of 17 August 1999 Izmit (Turkey) earthquake using radar interferometry: Geophysical Research Letters, v. 28, p. 1079-1082.

Yagi, Y., 2001, http://www.eic.eri.u-tokyo.ac.jp/yuji/English.html.

Yagi, Y., and Kikuchi, M., 2000, Source rupture process of the Kocaeli, Turkey, earthquake of August 17, 1999, obtained by joint inversion of near-field and teleseismic data: Geophysical Research Letters, v. 27, p. 1969-1972.

Yu, E., and Segall, P., 1996, Slip in the 1868 Hayward earthquake from the analysis of historical triangulation data: Journal of Geophysical Research, v. 101, p. 16,101-16,118.

Table D.1. Wells and Coppersmith (1994) Strike Slip Earthquakes

Earthquake	W&C #	M	Moment	Length	Width
1906 San Francisco	7	7.9	7.90E+27	432	12
1932 Long Beach	21	6.38	4.10E+25	23	13
1940 Imperial V.	26	6.92	2.70E+26	45	11
1958 Lituya Bay	53	7.77	5.10E+27	350	12
1963 Wakasa Bay	57	6.28	3.00E+25	20	8
1963 Skopje	58	5.99	1.10E+25	17	11
1966 Parkfield	63	6.25	2.70E+25	35	10
1966 Truckee	66	5.96	9.70E+24	13	7
1968 Borrego Mtn.	71	6.63	1.00E+26	40	10
1968 Dasht-e-Bayaz	73	7.23	7.80E+26	110	20
1968 Rampart	75	6.69	1.20E+26	30	8
1969 Coyote Mtn.	77	5.69	3.80E+24	10	3
1969 Gifu	80	6.34	3.60E+25	18	10
1969 Ceres	81	6.37	4.00E+25	20	9
1972 Sitka	91	7.7	4.00E+27	180	10
1973 Luho	96	7.47	1.80E+27	110	13
1974 Izu-Oki	100	6.54	7.20E+25	18	11
1975 Haicheng	104	6.99	3.45E+26	60	15
1975 Oita	106	6.32	3.40E+25	10	10
1976 Guatamala	112	7.63	3.10E+27	257	13
1976 Tangshan	116	7.46	1.76E+27	70	24
1976 Songpan #1	117	6.71	1.30E+26	30	12
1976 Songpan #3	120	6.58	8.40E+25	22	11
1976 Mexico	122	5.61	2.90E+24	9	5
1977 Bob-Tangol	128	5.89	7.60E+24	14	12
1978 Izu-Oshima	129	6.71	1.32E+26	50	10
1979 Homesead V	138	5.55	2.41E+24	6	4
1979 Coyote L.	141	5.77	5.10E+24	14	10
1979 Imperial V.	144	6.53	7.12E+25	51	12
1980 Mammoth L. #4	151	5.99	1.09E+25	9	11
1980 Mexicali	152	6.4	4.50E+25	28	8
1980 Izu-Hanto-Toho	153	6.39	4.30E+25	14	10
1981 Daofu	158	6.64	1.01E+26	46	15
1983 Pasinier	175	6.73	1.40E+26	50	16
1983 Guinea	177	6.32	3.40E+25	27	14
1984 Morgan Hill	178	6.28	3.00E+25	26	8
1974 Naganoken-Seibu	183	6.24	2.60E+25	12	8
1984 Round V.	185	5.83	6.20E+24	7	7
1985 New Britan	187	7.19	6.93E+26	50	15
1985 Algeria	192	6	1.11E+25	21	13
1986 Mt. Lewis	198	5.64	3.20E+24	5.5	4
1986 N. Palm Sp.	201	6.13	1.73E+25	16	9
1986 Chalfant V.	203	6.31	3.20E+25	20	11
1987 Elmore Ranch	215	6.2	2.60E+25	30	12
1987 Superstition H.	216	6.61	9.20E+25	30	11
1988 Lancang-Gengma	221	7.13	5.47E+26	80	20
1989 Loma Prieta	227	6.92	2.67E+27	40	16
1990 Izu-Oshima	230	6.37	4.05E+25	19	12
1990 Luzon	233	7.74	4.60E+27	120	20
1992 Joshua Tree	239	6.27	2.90E+25	15	13
1992 Landers	240	7.34	1.14E+27	62	12
1992 Big Bear	241	6.68	1.16E+26	20	10

Table D.2. California Earthquake Ruptures with Geologic and Geodetic Data

Earthquake	M	Length	Width	Source
1857 Ft. Tejon	7.83	300	13	Sieh (1978)
1868 Hayward	6.95	52	10	Yu and Segall (1996)
1868 Hayward	7.05	52	15	Yu and Segall (1996)
1872 Owens V.	7.6	110	15	Beanland and Clark (1994)
1872 Owens V.	7.46	110	12.5	Stein and Hanks (1998)
1906 San Francisco	7.88	470	10	Thatcher et al. (1997)
1940 Imperial V.	6.97	65	9	King and Thatcher (1998)
1989 Loma Prieta	6.95	37	13	Lisowski et al. (1990)
1989 Loma Prieta	6.95	36	10	Arnadottir et al. (1992)
1992 Landers	7.31	65	10	Hudnut et al. (1994)
1992 Landers	7.27	65	10	Freymueller et al. (1994)

Table D.3. Strike Slip Earthquake Rupture Models from Sommerville, et al. (1999)

Earthquake	Length	Width	M
1979 Coyote Lake	5.5	4.57	5.66
1979 Imperial Valley	36	10	6.43
1984 Morgan Hill	26	11.5	6.18
1986 North Palm Springs	20	13.3	6.14
1987 Superstition Hills	20	8.05	6.33
1989 Loma Prieta	40	18	6.95
1992 Landers	69	15	7.22
1995 Kobe	60	20	6.9

Table D.4. Earthquakes added from literature or unpublished studies

Earthquake	M	Moment	Length	Width	Source
1905 Bunlay, Mongolia	7.97	1.00E+28	300	15	Schwartz, written comm. (2001)
1905 Bunlay, Mongolia	8.1	1.70E+28	350	20	Schwartz, written comm. (2001)
1939 Erzihcan, Turkey	7.9	5.20E+27	327	12.5	Barka (1996); Stein et al. (1997)
1942 Erbaa, Turkey	6.9	1.70E+26	40	12.5	Barka (1996); Stein et al. (1997)
1943 Kastamonu, Turkey	7.7	2.90E+27	275	12.5	Barka (1996); Stein et al. (1997)
1944 Bolu, Turkey	7.5	1.50E+27	162	12.5	Barka (1996); Stein et al. (1997)
1949 Elmalidere, Turkey	7.1	3.50E+26	63	12.5	Barka (1996); Stein et al. (1997)
1951 Turkey	6.8	1.40E+26	35	16.25	Barka (1996); Stein et al. (1997)
1957 Abant, Turkey	6.8	1.40E+26	27	12.5	Barka (1996); Stein et al. (1997)
1957 Gobi Altai, Mongolia	7.71	4.20E+27	260	15	Schwartz, written comm. (2001)
1957 Gobi Altai, Mongolia	8.04	1.30E+28	260	20	Molnar and Chen (1977)
1966 Varto, Turkey	6.6	6.00E+25	41	12.5	Barka (1996); Stein et al. (1997)
1967 Mudurna V., Turkey	7	2.70E+26	75	12.5	Barka (1996); Stein et al. (1997)
1971 Bingol, Turkey	6.8	1.20E+26	51	12.5	Barka (1996); Stein et al. (1997)
1992 Erzincan, Turkey	6.5	4.00E+25	20	12.5	Barka (1996); Stein et al. (1997)
1996 Manyi, Tibet	7.6	2.80E+27	170	8	Peltzer et al. (1999)
1999 Izmit, Turkey	7.4	2.60E+27	136	12.5	Wright et al. (2001)
1999 Izmit, Turkey	7.58	2.60E+27	150	17	Delouis et al. (2000)
1999 Izmit, Turkey	7.4	1.40E+27	70	15	Yagi and Kikuchi (2000)
1999 Hector Mine	7.1	5.00E+26	54	13	Ji, et al., (in press)
1999 Hector Mine	7.1	6.10E+26	42	18	Yagi (2001)
1999 Duzce, Turkey	7.1	4.50E+26	40	12.5	Akyuz et al. (2000)
1999 Duzce, Turkey	7.1	5.60E+26	30	20	Yagi (2001)
2000 Tottori, Japan	6.6	1.10E+26	22	12	Yagi (2001)
2000 New Ireland, P.N.G.	8	1.30E+28	210	40	Yagi (2001)

Figure Captions

Figure D.1. Rupture area (A) in km^2 versus moment magnitude (**M**).

Figure D.2 Moment magnitude versus mean slip (U) in cm. Mean slip determined from definition of seismic moment using reported **M**, A, and shear modulus of 3_10^{11} dynes/cm^2.

Figure D.3. Rupture length (L) in km versus mean slip (U) in cm.

Figure D.4. Rupture length in km versus stress drop. Stress drop defined at the center of a rectangular dislocation with constant slip that intersects the free surface.

Figure D.5. Effect of random measurement (epistemic) errors in A and **M** on a hypothetically observed rupture of each WG99 rupture source. The correct value of $\log_{10}(A)$ for each rupture source has been corrupted by the addition of Gaussian noise with a s.d. of 0.15. Similarly, the correct values of M determined using equation (2.6b) were corrupted with Gaussian noise with a s.d. of 0.08. If measurements were error free, they would all fall on the solid line. The dashed and dotted lines correspond to 90% range of a hypothetical aleatory variability of **M** equal to 0.12 and 0.25, respectively.

Figure D.1

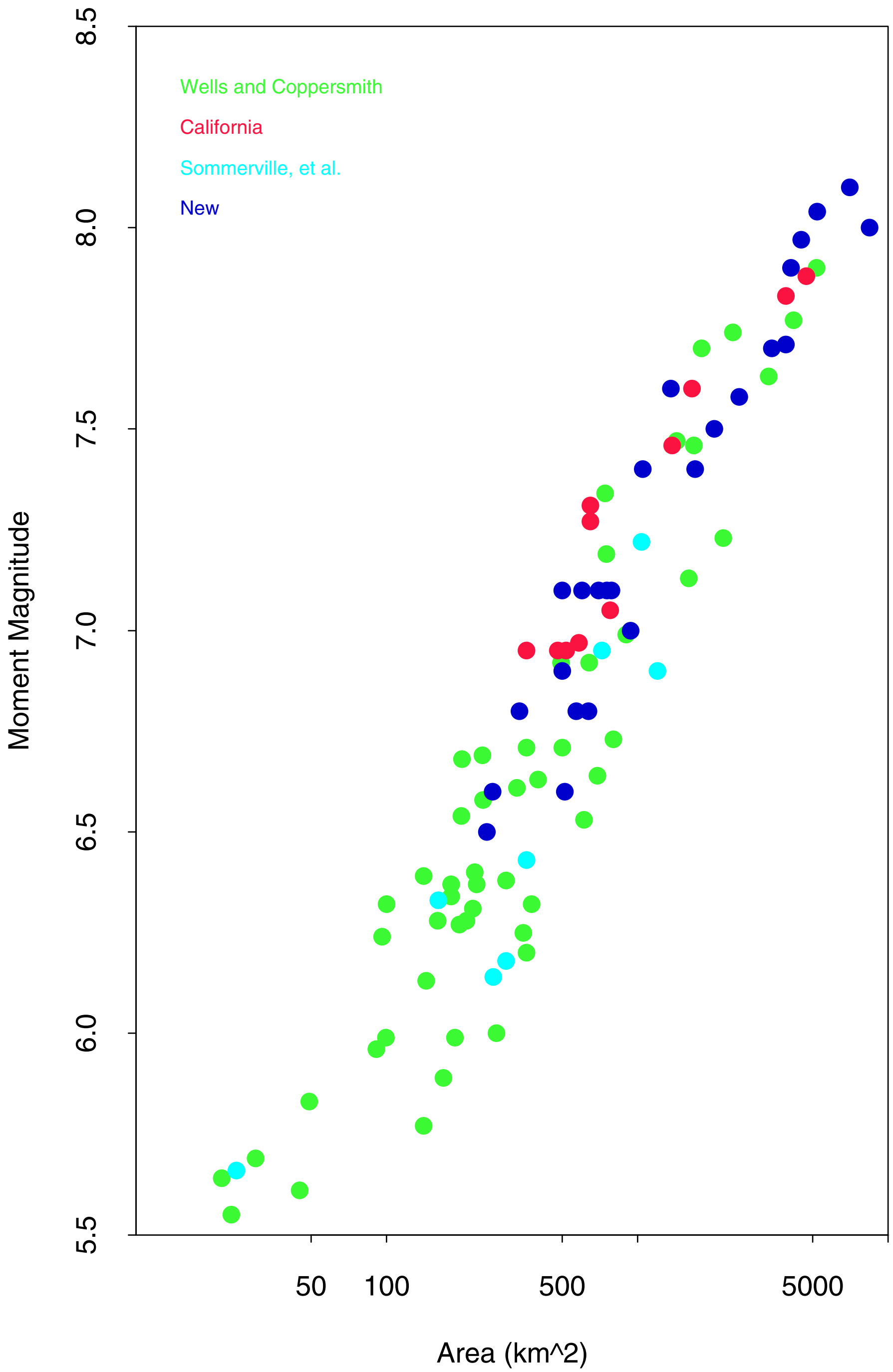

Figure D.2

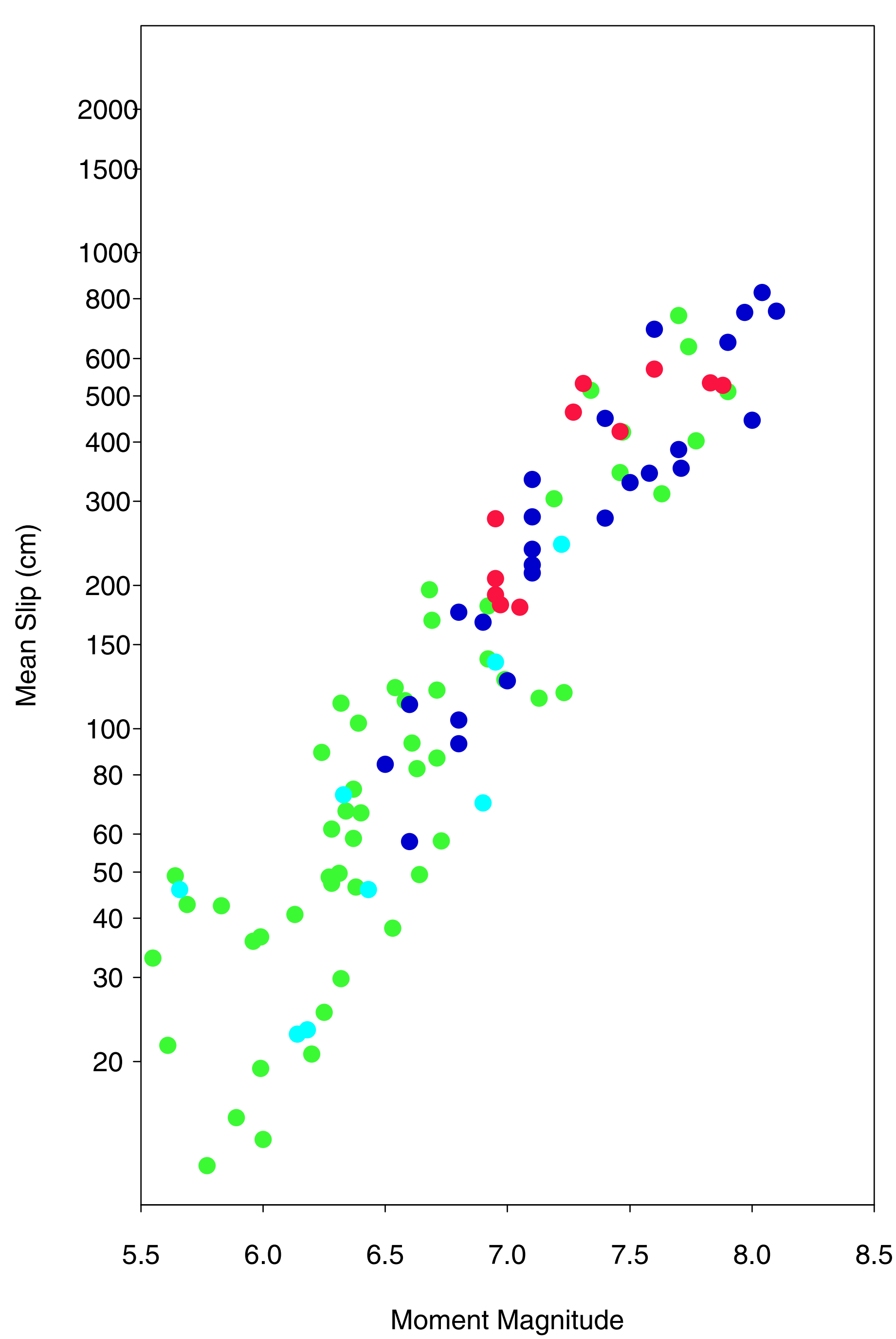

Figure D.3

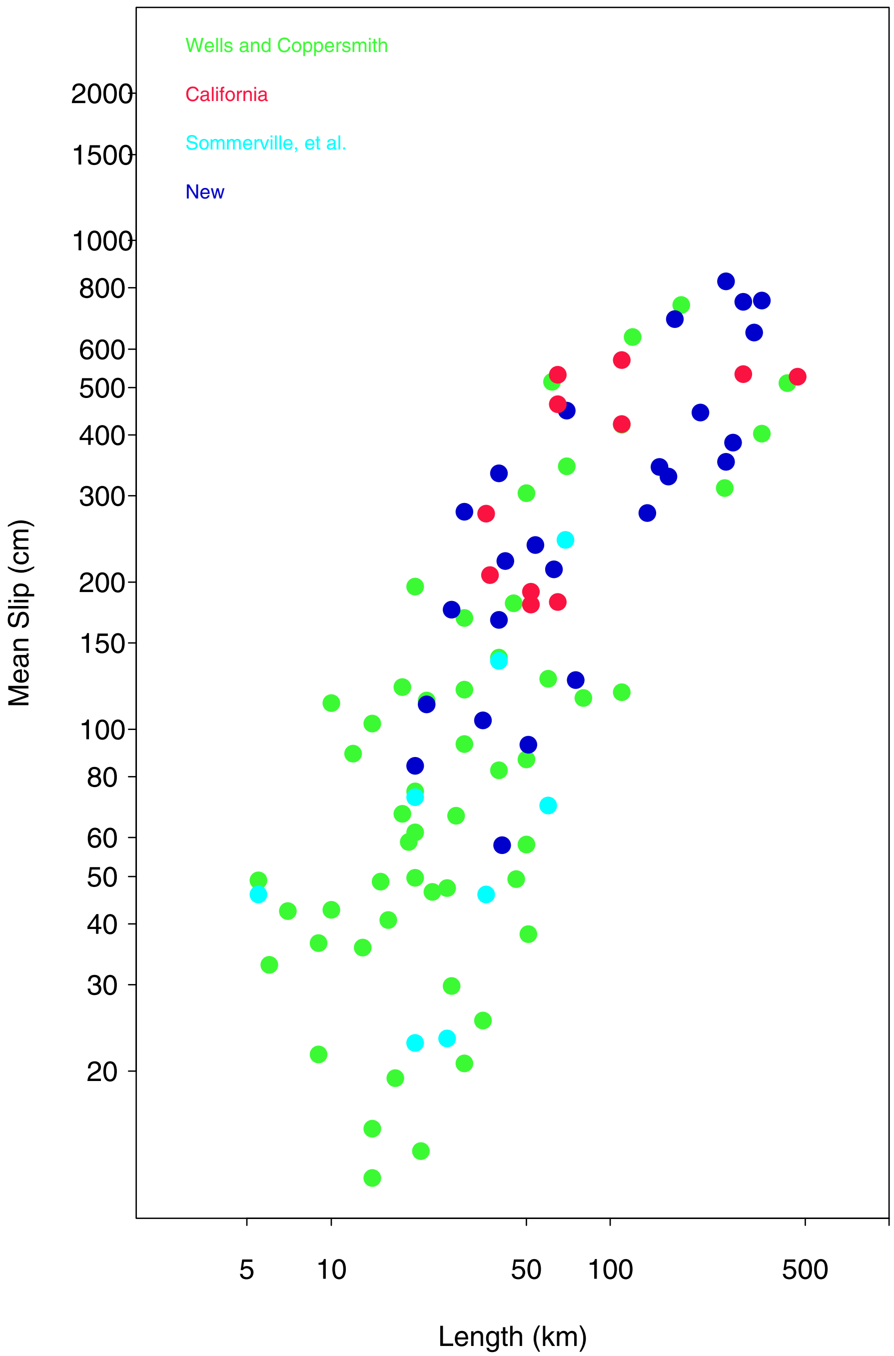

Figure D.4

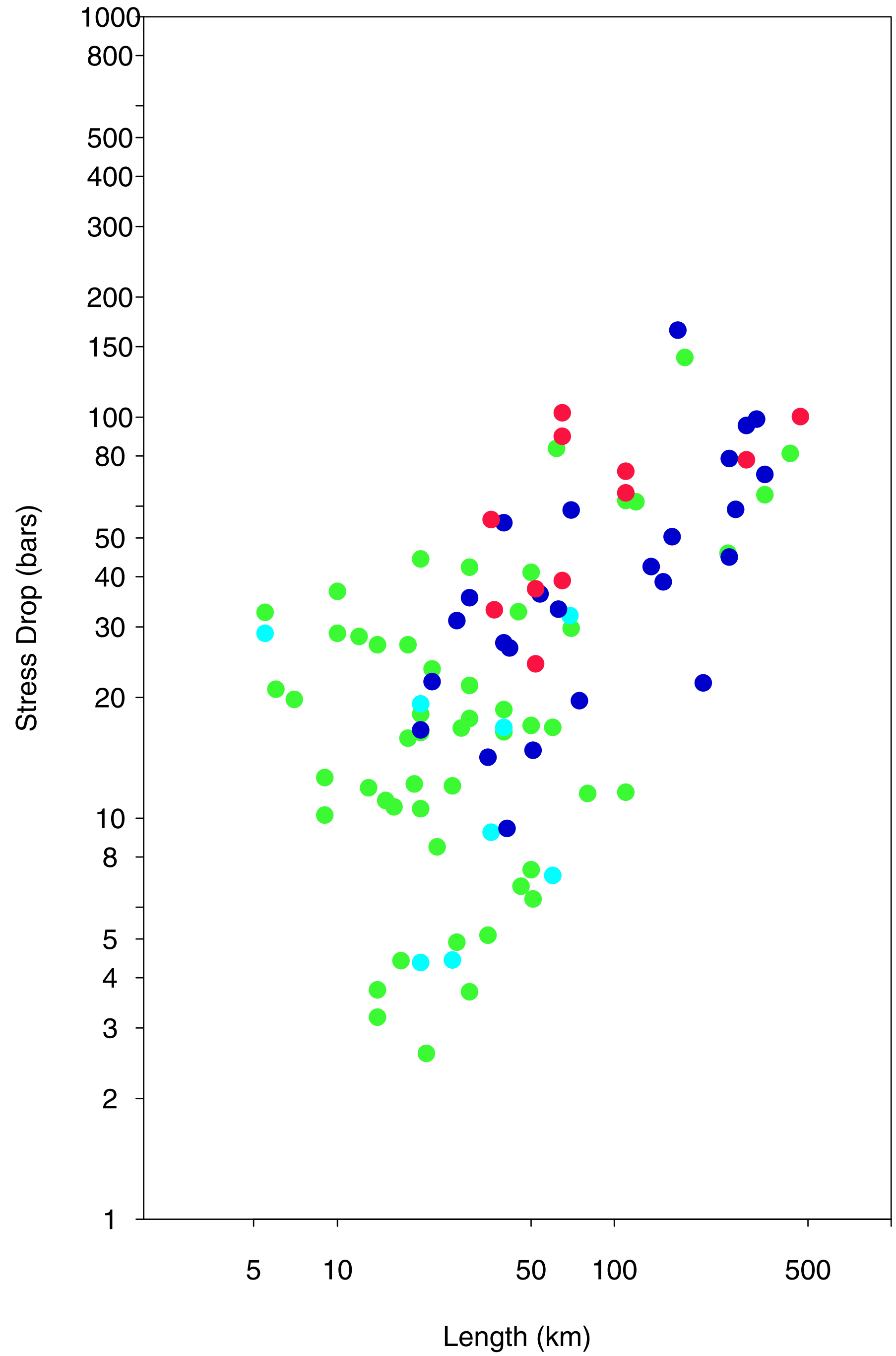

Figure D.5